Eur. Phys. J. A **16**, 475–487 (2003)
DOI 10.1140/epja/i2001-10273-1

THE EUROPEAN PHYSICAL JOURNAL A

Some considerations on the restoration of Galilei invariance in the nuclear many-body problem

Part IV: Simple continuum states

K.W. Schmid[a]

Institut für Theoretische Physik der Universität Tübingen, Auf der Morgenstelle 14, D-72076 Tübingen, Germany

Received: 20 February 2001 /
Published online: 25 March 2003 –
Communicated by D. Schwalm

Abstract. The effects of the restoration of Galilei invariance on many-nucleon states with one nucleon in the continuum are investigated within a simple knock-out model for quasi-elastic electron scattering using a Woods-Saxon partial-wave expansion for the continuum nucleon and simple Slater determinants for the bound states. For the total longitudinal response functions of the three nuclei ^{4}He, ^{16}O and ^{40}Ca, as seen in inclusive experiments, a rather good agreement of the Galilei-invariant prescription and the usual spectral-function approximation is obtained, provided that in the latter the momentum transfer is quenched by a factor $(A-1)/A$, and furthermore relative motion wave functions are used for the various hole states. The agreement is worse if exclusive scattering is considered. Then the above modifications of the spectral-function approximation still yield the right positions and shapes for the partial longitudinal response functions of the various residual hole states. However, as expected from the different spectroscopic factors obtained for the Galilei invariant with respect to the normal approximation in the first of the present series of papers, for holes out of the last occupied shell the corrected spectral-function approach underestimates the Galilei-invariant strengths, while for holes from the lower shells a considerable overestimation of the strengths is observed.

PACS. 21.60.-n Nuclear-structure models and methods

1 Introduction

Galilei invariance requires that the effective Hamiltonian describing an A-nucleon system in its center-of-momentum (COM) rest frame does neither depend on the center-of-mass coordinate nor on the total linear momentum of the constituents. The nuclear many-body problem is hence to solve the corresponding A-nucleon Schroedinger equation for wave functions depending only on relative coordinates, too. But nucleons are fermions and thus their wave function has to be antisymmetric. The relative coordinates, however, depend on all the nucleon coordinates and thus the antisymmetrisation has to be done explicitly. For few-body systems this is no problem and consequently the text-book description of the deuteron, the Fadeev equations for the three-, or the Fadeev-Jakubowski equations for the four-body system use this procedure. For eight or even more like nucleons, on the other hand, this procedure becomes impractical. Thus, in the nuclear many-body problem one usually expands the wave function in terms of Slater or generalized Slater determinants. In this way the Pauli principle is respected explicitly, however, depending on $3A$ instead of the allowed $(3A-3)$ coordinates, such wave functions massively break the Galilei invariance.

In the first three of the present series of papers [1–3] it was demonstrated how the Galilei invariance of bound many-nucleon states can be restored by applying the projection operator

$$\hat{C}_A(0) \equiv \int \mathrm{d}^3\,\vec{a}\,\hat{S}_A(\vec{a}) \equiv \int \mathrm{d}^3\,\vec{a}\,\exp\{i\vec{a}\cdot\hat{P}_A\}\,, \quad (1.1)$$

where

$$\hat{P}_A \equiv \sum_{i=1}^{A}\hat{p}_i\,, \quad (1.2)$$

is the total linear momentum operator of the considered A-nucleon system.

This operator projects into the center-of-momentum (COM) rest frame of the considered A-nucleon system by superposing the states obtained by shifting the wave function to all points in ordinary space with equal weight. Obviously, the convergence of this procedure requires that the wave function is localized. Thus the restoration of translational invariance (or full Galilei invariance, if the

[a] e-mail: karl-wilhelm.schmid@uni-tuebingen.de

projection is done before the wave function is dynamically determined, *e.g.*, by variation) via the operator (1.1) is only possible for bound states.

Simple examples for such bound states (the oscillator ground states of ^{4}He, ^{16}O and ^{40}Ca as well as all the one-hole states with respect to these reference configurations) have been studied extensively in [1–3]. Spectral functions and spectroscopic factors [1], form factors for elastic and inelastic electron scattering between bound states [2], sum rules [2], and finally energies obtained for effective interactions without and with density-dependence [3] have been investigated. In contradiction to the general belief, in most of these examples the exact restoration of Galilei invariance produced results which were considerably different from those obtained by the usual approximate methods to treat the COM motion.

In the present paper the investigation will be extended to simple scattering states with one nucleon in the continuum. The corresponding wave function is not localized any more but oscillating at infinity. Thus, for the treatment of continuum problems, the use of (1.1) alone is not sufficient. As will be shown in the following, the restoration of Galilei invariance is nevertheless straightforward and can be achieved using exactly the same mathematical methods developed in [1].

In conventional nuclear physics one usually does not care about Galilei invariance and expands an A-nucleon scattering state with one nucleon in the continuum in terms of partial channels of the form

$$|C_\alpha(E); A\,T_z = T_z^\alpha + \tau;\,[lj, I_\alpha]I_c M_c\rangle \equiv \sum_{\lambda\,\sigma\,m\,M_\alpha} \left(l\frac{1}{2}j|\lambda\sigma m\right)(jI_\alpha I_c|mM_\alpha M_c) \cdot \int \mathrm{d}kk^2 \left\{ \int \mathrm{d}\Omega_k\, Y^*_{l\lambda}(\Omega_k)\, c^\dagger_{\vec{k}\,\tau\sigma} |\Psi^{\alpha\,T_z^\alpha}_{A-1};\, I_\alpha M_\alpha\rangle \right\} g^E_{\alpha\tau lj}(k)\,, \tag{1.3}$$

in which a partial wave with quantum numbers τlj is coupled to some bound state α of the $(A-1)$-nucleon system. The operator

$$c^\dagger_{\vec{k}\,\tau\sigma}|0\rangle \equiv |\vec{k}\rangle|\tau\sigma\rangle \tag{1.4}$$

creates a plane-wave nucleon with momentum $\hbar\vec{k}$ and isospin- and spin-projections τ and σ from the particle vacuum. Expression (1.3) is the momentum representation of the channel. The expansion coefficients $g^E_{\alpha\tau lj}(k)$ can be obtained by either a potential scattering approach (*e.g.*, Woods-Saxon partial waves) or, more microscopic, by some coupled-channel calculation using some suitable many-body Hamiltonian. The first case will be studied in the present paper, the second in the next of the present series of papers. If in the potential scattering approach the same potential is used to create bound and scattering single-particle states, then the channels (1.3) are orthogonal to all the bound states of the A-nucleon system.

Obviously, an expansion in the channels (1.3) is not Galilei invariant. First of all, the bound states α of the residual nucleus do not live in their COM rest frame, but are usually, as already mentioned, a linear combination of Slater or generalized Slater determinants which massively break this symmetry. Thus, instead of $|\Psi^{\alpha\,T_z^\alpha}_{A-1};\, I_\alpha M_\alpha\rangle$ the projected states

$$|\Psi^{\alpha\,T_z^\alpha}_{A-1};\, I_\alpha M_\alpha;\,(0)\rangle \equiv \frac{\hat{C}_{A-1}(0)|\Psi^{\alpha\,T_z^\alpha}_{A-1};\, I_\alpha M_\alpha\rangle}{\sqrt{\langle\Psi^{\alpha\,T_z^\alpha}_{A-1};\, I_\alpha M_\alpha|\hat{C}_{A-1}(0)|\Psi^{\alpha\,T_z^\alpha}_{A-1};\, I_\alpha M_\alpha\rangle}} \tag{1.5}$$

should be used for the description of the residual nucleus.

Second, an expansion in terms of (1.3) does not yield the desired asymptotic behaviour. In fact, asymptotically the system should be described by a relative motion wave function for the outgoing (or incoming) nucleon with respect to the residual nucleus, while in (1.3) not relative but normal coordinates are used. In other words, in (1.3) the "recoil" of the $A-1$ system is neglected.

A Galilei-invariant description thus requires an Ansatz of the form

$$|C_\alpha(E); A\,T_z = T_z^\alpha + \tau;\,[lj, I_\alpha]I_c M_c;\,(0)\rangle \equiv \sum_{\lambda\,\sigma\,m\,M_\alpha} \left(l\frac{1}{2}j|\lambda\sigma m\right)(jI_\alpha I_c|mM_\alpha M_c) \cdot \int \mathrm{d}kk^2 \left\{ \int \mathrm{d}\Omega_k\, Y^*_{l\lambda}(\Omega_k)\, c^\dagger_{\vec{k}\,\tau\sigma} \cdot \exp\{-i\vec{k}\cdot\vec{R}_{A-1}\}|\Psi^{\alpha\,T_z^\alpha}_{A-1};\, I_\alpha M_\alpha;\,(0)\rangle \right\} g^E_{\alpha\tau lj}(k)\,, \tag{1.6}$$

which now yields the desired asymptotics. The price one has to pay is the occurence of the $(A-1)$-body recoil operator $\exp\{-i\vec{k}\cdot\vec{R}_{A-1}\}$ as well as of the COM-projected state (1.4) in this Ansatz.

It should be stressed here that in general neither the configurations occuring in (1.3) nor those in (1.6) are orthogonal. For the potential scattering approach discussed in the present paper, however, the effects of these non-orthogonalities are small and can hence be neglected. This is not the case if the expansion coefficients in (1.3) and (1.6) are determined in a coupled-channel approach. There a careful orthonormalisation of the channels is unavoidable.

In the present paper we shall investigate the difference of the Galilei-invariant Ansatz (1.6) with respect to the conventional form (1.3) for the example of quasi-elastic electron scattering from the three nuclei ^{4}He, ^{16}O and ^{40}Ca. The expansion coefficients will be taken from potential scattering using a Woods-Saxon potential. The above-mentioned non-orthogonality effects will be neglected and, for simplicity, only the longitudinal response functions will be studied.

In the next of the present series of papers we shall then study a more microscopic coupled-channel approach to the problem. There both longitudinal and transverse response functions will be calculated and the channels will be properly orthonormalized.

2 A simple knock-out model

As an example for the effects obtained if instead of the normal description (1.3) the Galilei-invariant Ansatz (1.6) is used, we shall discuss in the following the longitudinal reponse function for inelastic electron scattering in a simple knock-out model for the three target nuclei ^{4}He, ^{16}O and ^{40}Ca.

In the conventional ("normal") approach the ground states of these nuclei will be described by simple oscillator Slater determinants

$$|\,\rangle \;=\; \prod_{Hh} b^\dagger_{Hh}\,|0\rangle\,, \tag{2.1}$$

where the operator

$$b^\dagger_{Hh}|0\rangle \;\equiv\; |H\rangle|h\rangle \tag{2.2}$$

creates from the particle vacuum a nucleon with isospin- and spin-projections $h \equiv \tau_h, \sigma_h$ in an oscillator state with quantum numbers $H \equiv n_{Hx}n_{Hy}n_{Hz}$ in Cartesian or $H \equiv n_H l_H \lambda_H$ in spherical representation, respectively. The states of the residual nucleus will be described by the one-hole states with respect to (2.1)

$$\begin{aligned}|\Psi^\alpha_{A-1};\, I_\alpha M_\alpha\rangle \;\equiv\; & \delta_{\alpha H}\delta_{I_\alpha j_H}\delta_{M_\alpha - m_H}\,(-)^{j_H-m_H} \\ & \cdot \sum_{\lambda_H \sigma_h}\left(l_H \tfrac{1}{2} j_H|\lambda_H \sigma_h m_H\right) b_{Hh}|\,\rangle \end{aligned} \tag{2.3}$$

and for the continuum nucleon Woods-Saxon partial waves will be used. The Woods-Saxon potential has the form

$$\begin{aligned} V_{\tau lj}(r) \;\equiv\; & \frac{U_0}{1+\exp\{(r-R_0)/a_0\}} \\ & + \frac{U_{ls}}{m_\pi^2 a_{ls} r}\,\frac{\exp\{(r-R_{ls})/a_{ls}\}}{[1+\exp\{(r-R_{ls})/a_{ls}\}]^2} \\ & \times \begin{Bmatrix} l\,, & \text{for } j = l+1/2 \\ -(l+1)\,, & \text{for } j = l-1/2 \end{Bmatrix} \\ & + \delta_{\tau p}\, e^2 (Z-1) \\ & \times \begin{Bmatrix} 1/r\,, & \text{for } r > R_C \\ (1/2R_C)[3-(r/R_C)^2]\,, & \text{for } r \le R_C \end{Bmatrix}, \end{aligned} \tag{2.4}$$

where m_π is the mass of the pion and the radii are parametrized as usual by

$$R_\alpha \;\equiv\; r_\alpha\,(A-1)^{1/3} \tag{2.5}$$

for $\alpha = 0, ls, C$. Note, that the corresponding Schroedinger equation describes the *relative* motion of one nucleon in the field of the other $A-1$ nucleons and that hence the reduced mass of the problem has to be used in the kinetic-energy operator.

Obviously, in principle one should use the bound solutions of the potential (2.4) instead of harmonic-oscillator states to construct the target ground state (2.1) and the states of the residual system (2.3). It turns out, however, that after optimizing the oscillator length so that the sum of the overlaps of the oscillator states occupied in (2.1) with the corresponding Woods-Saxon solutions becomes maximal, (2.1) and (2.3) are excellent approximations to the corresponding Woods-Saxon determinants. We shall hence keep the oscillator representation of (2.1) and (2.3) which allows for an analytic evaluation of the various matrix elements discussed in the following and thus for greater transparency.

For the longitudinal response functions the matrix elements of the charge density operator between the target state (2.1) and the channels (1.3) have to be calculated. This operator can be written in momentum representation as [2]

$$\hat\rho^{\rm nor}(\vec q,\,\omega) \;\equiv\; \sum_{\tau_1} f_{\tau_1}(Q^2) \sum_{\sigma_1}\!\int \mathrm{d}^3\,\vec k_1\, c^\dagger_{\vec k\,\tau_1\sigma_1}\, c_{\vec k - \vec q\,\tau_1\sigma_1}\,, \tag{2.6}$$

where the nucleon charge form factors f_τ as usual are given by

$$f_\tau(Q^2) \;\equiv\; G^\tau_E(Q^2) \;-\; \frac{Q^2}{8M^2}\,\frac{G^\tau_E(Q^2) \,+\, \frac{Q^2}{4M^2} G^\tau_M(Q^2)}{1 \,+\, \frac{Q^2}{4M^2}} \tag{2.7}$$

with the Sachs form factors parametrized in the widely used dipole form (see, *e.g.*, Preston and Bhaduri [4])

$$\begin{aligned} G^p_E(Q^2) \;\equiv\; & \left[1 \,+\, \frac{Q^2}{(843\mathrm{MeV})^2}\right]^{-2}, \\ G^\tau_M(Q^2) \;\equiv\; & \mu_\tau\, G^p_E(Q^2) \qquad \text{with} \quad \begin{Bmatrix} \mu_p \;=\; +2.793 \\ \mu_n \;=\; -1.913 \end{Bmatrix}, \\ G^n_E(Q^2) \;\equiv\; & -\mu_n \frac{Q^2}{4M^2}\,\frac{1}{1 \,+\, 5.6\frac{Q^2}{4M^2}}\, G^p_E(Q^2)\,. \end{aligned} \tag{2.8}$$

They depend on the (negative) square of the 4-momentum transfer

$$Q^2 \;\equiv\; (\hbar c \vec q)^2 \;-\; (\Delta E)^2\,, \tag{2.9}$$

with $\Delta E \equiv \omega$ being the energy transfer to the system.

In our simple knock-out model we obtain easily

$$\begin{aligned} & \langle\, |b^\dagger_{Hh} C_{\vec k\, p}\, \hat\rho^{\rm nor}|\,\rangle \;= \\ & \Delta_{ph}\left\{ f_\tau \langle \vec k - \vec q\,|H\rangle + \sum_{H_1}\langle \vec k\,|H_1\rangle \langle\, |b^\dagger_{Hh}\hat\rho^{\rm nor} b_{H_1 p}|\,\rangle \right\} \end{aligned} \tag{2.10}$$

with $\Delta_{ph} \equiv \delta_{\tau_p\tau_h}\delta_{\sigma_p\sigma_h}$.

The first term is immediately recognized as the complex conjugate of the usual spectral function discussed already in [1]. For the simple ground state (2.1) one obtains the Fourier transform of the considered hole state at momentum $\vec k - \vec q$ multiplied with the charge form factor (2.7) of the nucleon. The corresponding spectroscopic factors equal unity for all the hole states.

The second term in (2.10) contains the scattering between the various hole states. The corresponding form factors have been derived in [2]. Each of the terms in the sum is multiplied by the Fourier transform of the hole state H_1 at momentum $\vec{k}$. If the partial waves entering the channels (1.3) were constructed from the same average potential as the bound states (2.2), then, because of orthogonality, the second term would not contribute at all and we are left with the spectral-function part. This "spectral-function approximation" is usually called the "distorted-wave impulse approximation (DWIA)". Since the outgoing nucleon feels the mean field of the other nucleons, one sometimes may argue that the DWIA takes into account (at least some of) the "final-state interaction" (FSI). It should, however, be stressed that the simple knock-out model presented here except for the "mean-field" contribution does not include any nucleon-nucleon correlations at all and is hence a rather simple independent particle model. Note furthermore that we do not use Woods-Saxon but oscillator wave functions for the bound states. Thus the above statement about the orthogonality is only approximately true. However, we shall see that this causes only very small deviations from the spectral-function approximation.

The expression (2.10) can be evaluated easily using the standard techniques presented in [1]. One obtains

$$\begin{aligned}\langle\, |b^{\dagger}_{Hh} C_{\vec{k}\,p}\hat{\rho}^{\rm nor}|\,\rangle \;=\; & \left(\frac{b}{\sqrt{\pi}}\right)^{3/2} \\ & \times \Delta_{ph}\Bigg\{\exp\left[-\frac{\kappa^2+\lambda^2}{2}+\vec{\kappa}\cdot\vec{\lambda}\right]\left(\vec{\kappa}-\vec{\lambda}|H\right) \\ & +\exp\left[-\frac{\kappa^2}{2}-\frac{\lambda^2}{4}\right]\Bigg[(\vec{\kappa}|H)\,2[f_\tau+f_{-\tau}]\,\frac{1}{\pi\sqrt{\pi}} \\ & \times\int \mathrm{d}^3\,\vec{z}\,\exp[-z^2]\,y\left(\vec{z}-\frac{1}{2}\vec{\lambda},\,\vec{z}+\frac{1}{2}\vec{\lambda}\right) \\ & -f_\tau\,\frac{1}{\pi\sqrt{\pi}}\int \mathrm{d}^3\,\vec{z}\,\exp[-z^2]\,y \\ & \times\left(\vec{\kappa},\,\vec{z}+\frac{1}{2}\vec{\lambda}\right)\left(\vec{z}-\frac{1}{2}\vec{\lambda}|H\right)\Bigg]\Bigg\}, \end{aligned} \tag{2.11}$$

where $\tau \equiv \tau_p \equiv \tau_h$, b is the oscillator length, $\vec{\kappa} \equiv b\vec{k}$ and $\vec{\lambda} \equiv b\vec{q}$. $(\vec{a}|H)$ are the polynomial parts of the oscillator states $|H\rangle$ in (dimensionless) momentum representation. For the three nuclei considered here they are given in [1] as well as the functions

$$y(\vec{z}_2,\,\vec{z}_1) \;\equiv\; \sum_H (\vec{z}_2|H)(H|\vec{z}_1)\,. \tag{2.12}$$

For the Galilei-invariant channels (1.6) now instead of (2.1) the COM-projected ground state

$$|\,,\,(0)\rangle \;\equiv\; \hat{C}_A(0)|\,\rangle\left(\frac{A}{4\pi b^2}\right)^{3/4} \tag{2.13}$$

has to be used and for the residual nucleus the states (2.3) have to be replaced by the corresponding COM-projected one-hole states (angular-momentum coupling supressed for simplicity). As derived in [1] these are

$$\begin{aligned}|(Hh)^{-1},\,(0)\rangle \;\equiv\; & \hat{C}_{A-1}(0)b_{Hh}|\,\rangle\left(\frac{A-1}{4\pi b^2}\right)^{3/4} \\ & \times\left\{\begin{array}{ll} 1\,, & \text{for } H=0s \text{ in } {}^4\mathrm{He} \\ 1\,, & \text{for } H=0p\lambda \text{ in } {}^{16}\mathrm{O} \\ \sqrt{\frac{5}{4}}\,, & \text{for } H=0s \text{ in } {}^{16}\mathrm{O} \\ 1\,, & \text{for } H=1s \text{ in } {}^{40}\mathrm{Ca} \\ 1\,, & \text{for } H=0d\lambda \text{ in } {}^{40}\mathrm{Ca} \\ \sqrt{\frac{39}{35}}\,, & \text{for } H=0p\lambda \text{ in } {}^{40}\mathrm{Ca} \end{array}\right\}, \end{aligned} \tag{2.14}$$

while for the (with respect to the $1s$ hole) Gram-Schmidt orthogonalized $0\tilde{s}$ hole in ^{40}Ca

$$\begin{aligned}&|(0\tilde{s},h)^{-1},\,(0)\rangle \;\equiv\; \hat{C}_{A-1}(0) \\ &\times\left(b_{0s0h}|\,\rangle\sqrt{\frac{1014}{940}}+b_{1s0h}|\,\rangle\frac{1}{\sqrt{940}}\right)\left(\frac{A-1}{4\pi b^2}\right)^{3/4} \end{aligned} \tag{2.15}$$

has to be taken.

Furthermore, instead of the normal charge density operator (2.6) now the translational invariant form

$$\hat{\rho}^{\rm inv}_A(\vec{q},\,\omega) \;\equiv\; \hat{\rho}^{\rm nor}_A(\vec{q},\,\omega)\,\exp\{-i\vec{q}\cdot\vec{R}_A\} \tag{2.16}$$

has to be applied, in which the so-called Gartenhaus-Schwartz operator $\exp\{-i\vec{q}\cdot\vec{R}_A\}$ ensures that all coordinates are measured with respect to the center-of-mass coordinate $\vec{R}_A$ so that in (2.16) only relative coordinates do occur.

Using the techniques developed in [1], the Galilei-invariant form of the matrix element (2.11) can then be written as

$$\begin{aligned}&\langle(Hh)^{-1},\,(0)|\exp\{i\vec{k}\cdot\vec{R}_{A-1}\} \\ &\times c_{\vec{k}\,p}\,\hat{\rho}^{\rm nor}\,\exp\{-i\vec{q}\cdot\vec{R}_A\}|\,,\,(0)\rangle \;=\; \left(\frac{b\sqrt{\frac{A}{A-1}}}{\sqrt{\pi}}\right)^{3/2} \\ &\quad\times\Delta_{ph}\left\{\exp\left[-\frac{1}{2}\frac{A}{A-1}\kappa^2-\frac{1}{2}\frac{A-1}{A}\lambda^2+\vec{\kappa}\cdot\vec{\lambda}\right]\right. \end{aligned}$$

$$\cdot f_\tau \frac{1}{\pi\sqrt{\pi}} \int \mathrm{d}^3\,\vec{y}\,\exp\{-y^2\} r_H(\vec{\gamma}\,'_p,\,\vec{\gamma})$$

$$+ \exp\left[-\frac{1}{2}\frac{A}{A-1}\kappa^2 - \frac{1}{4}\frac{(A-1)^2+1}{(A-1)^2}\right.$$

$$\left.\cdot\frac{A-1}{A}\lambda^2 - \frac{1}{A-1}\vec{\kappa}\cdot\vec{\lambda}\right]$$

$$\cdot \frac{1}{\pi\sqrt{\pi}} \int \mathrm{d}^3\,\vec{u}\,\exp[-u^2]\,\frac{1}{\pi\sqrt{\pi}} \int \mathrm{d}^3\,\vec{w}\,\exp[-w^2]$$

$$\cdot \left[2[f_\tau + f_{-\tau}]\,x(\vec{\beta}\,'_2,\,\vec{\beta}_1)\,r_H(\vec{\beta}\,'_p,\,\vec{\beta})\right.$$

$$\left. - f_\tau\,x(\vec{\beta}\,'_p,\,\vec{\beta}_1)\,r_H(\vec{\beta}\,'_2,\,\vec{\beta})\right]\Bigg\}\,n_H\,, \qquad (2.17)$$

with the normalisation factors n_H given by eq. (2.14) for the one-hole states listed there, while for the $0\tilde{s}$ hole in ^{40}Ca the linear combination (2.15) of (2.17) for $H = 0s$ and $H = 1s$ has to be taken. By definition, in (2.17)

$$\begin{aligned}
\vec{\gamma} &\equiv \sqrt{\frac{2}{A-1}}\,\vec{y}\,,\\
\vec{\gamma}\,'_p &\equiv \sqrt{\frac{2}{A-1}}\,\vec{y} + i\sqrt{2}\frac{A}{A-1}\left(\vec{\kappa} - \frac{A-1}{A}\,\vec{\lambda}\right),\\
\vec{\beta} &\equiv \sqrt{\frac{2}{A-1}}\,\vec{u} + \frac{i}{\sqrt{2}}\frac{1}{A-1}\,\vec{\lambda}\,,\\
\vec{\beta}\,'_p &\equiv \sqrt{\frac{2}{A-1}}\,\vec{u} + i\sqrt{2}\frac{A}{A-1}\left(\vec{\kappa} + \frac{1}{2A}\,\vec{\lambda}\right),\\
\vec{\beta}_1 &\equiv -i\sqrt{2}\,\vec{w} + \frac{i}{\sqrt{2}}\,\vec{\lambda}\,,\\
\vec{\beta}\,'_2 &\equiv -i\sqrt{2}\,\vec{w} - \frac{i}{\sqrt{2}}\,\vec{\lambda}\,, \qquad (2.18)
\end{aligned}$$

and the functions x and r_H are polynomials in their arguments. They have been given for the three nuclei considered here explicitly in [1].

Again we can identify the first term as the projected spectral-function term discussed already in [1]. It can be written in shorthand notation

$$f_\tau(Q^2)\,\langle\vec{k} - \frac{A-1}{A}\vec{q}\,|(H)_{\mathrm{rel}}\rangle\,\sqrt{S_H^{\mathrm{pro}}} \qquad (2.19)$$

as the product of the nucleon charge form factor (2.7), the Fourier transform of the relative oscillator state $|(H)_{\mathrm{rel}}\rangle$ at momentum $\vec{k} - (A-1)\vec{q}/A$ and the square root of the corresponding spectroscopic factor

$$S_H^{\mathrm{pro}} = \left\{\begin{array}{ll}
1\,, & \text{for } H = 0s \text{ in } ^4\mathrm{He}\\
\frac{4}{5}\,, & \text{for } H = 0s \text{ in } ^{16}\mathrm{O}\\
\frac{16}{15}\,, & \text{for } H = 0p \text{ in } ^{16}\mathrm{O}\\
\frac{1410}{1521}\,, & \text{for } H = 0\tilde{s} \text{ in } ^{40}\mathrm{Ca}\\
\frac{1400}{1521}\,, & \text{for } H = 0p \text{ in } ^{40}\mathrm{Ca}\\
\frac{1600}{1521}\,, & \text{for } H = 1s \text{ in } ^{40}\mathrm{Ca}\\
\frac{1600}{1521}\,, & \text{for } H = 0d \text{ in } ^{40}\mathrm{Ca}
\end{array}\right\} \qquad (2.20)$$

as derived in [1]. The values in (2.20) are identical to those derived by Dieperink and de Forest [5] using different methods than applied here. The "relative" oscillator state can be obtained from the usual one by simply replacing the mass of the nucleon by the reduced mass of the 1 plus $(A-1)$ nucleon problem, or, equivalent, by modifying the oscillator length b into

$$\bar{b} \equiv b\sqrt{\frac{A}{A-1}}\,. \qquad (2.21)$$

Note, that in (2.19) the momentum $\vec{k} - (A-1)\vec{q}/A$, and not $\vec{k} - \vec{q}$ as in the normal description (2.11), is occuring. If we introduce

$$\begin{aligned}
\bar{\kappa} &\equiv \bar{b}\,k\,,\\
\bar{q} &\equiv \frac{A-1}{A}\,q\,,\\
\bar{\lambda} &\equiv \bar{b}\bar{q} = \sqrt{\frac{A-1}{A}}\,\lambda\,, \qquad (2.22)
\end{aligned}$$

then in these new variables the projected spectral-function part (2.19) gets the same functional form as the normal expression in (2.11) except that the spectroscopic factors are not equal to unity but given by (2.20).

The second term in (2.17) looks again rather similar to the second term in (2.11); however, here the orthogonality argument does not hold even if bound and scattering states are constructed from the same potential. This is due to the fact that the relative momentum $\vec{k}$ of the outgoing nucleon is modified if commuting the corresponding plane-wave annihilator with the Gartenhaus-Schwartz operator. Thus, the second term does always contribute here, though, as we shall see in the next chapter, its contributions are again rather small.

If we take only the spectral-function part of (2.11) into account but make the above modifications (2.21) and (2.22) we refer to this as the "corrected" spectral-function approximation. It differs from the full Galilei-invariant result (2.17) by the absence of the second term and by replacing the square roots of the spectroscopic factors (2.20) all by ones. Comparing the corrected spectral-function approximation with the Galilei-invariant result

thus gives an idea on the importance of the second term in (2.17) as well as of the effects of the spectroscopic factors (2.20).

We proceed by evaluating (2.11) and (2.17) using the Cartesian representation of b_{Hh} and then transforming the hole states into the spherical basis using the unitary tranformations given in [1]. Then the integration over $\mathrm{d}\Omega_k$ is performed in order to pick out a particular partial wave for the continuum nucleon. Afterwards we do the necessary angular-momentum coupling.

We furthermore choose, as usual, the direction of the momentum transfer $\vec{q}$ along the z-axis and define the energy loss of the electron as

$$\omega \equiv \epsilon + E_H - E_0 + E_{\rm rec}\,, \tag{2.23}$$

where ϵ is the (relative) kinetic energy of the outgoing nucleon, $E_H - E_0$ the threshold for removing a continuum nucleon from the A-nucleon ground state and leaving the residual nucleus in the state H, and

$$E_{\rm rec} \equiv \frac{(\hbar c)^2 q^2}{2AMc^2} \tag{2.24}$$

is the recoil energy of the system.

Taking finally into account that the plane-wave states are normalized to a three-dimensional Dirac delta-function in the wave vectors, while the Woods-Saxon partial waves are normalized to a delta-function in the energies, we obtain for the normal channels (1.3)

$$\begin{aligned}\langle C_\tau(\omega)\,[lj,n_Hl_Hj_H]IM|\,\hat\rho^{\rm nor}|\,\rangle \,=\,&\\ \delta_{M0}\,(-i)^{2n_H+l_H}\sqrt{\frac{4}{\hbar\omega_0}\sqrt{\frac{2\epsilon}{\pi\hbar\omega_0}}}&\\ \cdot\int \mathrm{d}k k^2\; F^{{\rm nor},\,\tau}_{[lj,n_Hl_Hj_H]I0}(k,q)\,g^\epsilon_{\tau lj}(k)\,,&\end{aligned} \tag{2.25}$$

where

$$\hbar\omega_0 \equiv \frac{(\hbar c)^2}{2Mc^2}\,\frac{A}{A-1}\,\frac{1}{b^2}\,, \tag{2.26}$$

while for the Galilei-invariant channels (1.6) one gets

$$\begin{aligned}\langle C_\tau(\omega);\,[lj,n_Hl_Hj_H]IM;\,(0)|\,\hat\rho^{\rm inv}|\,\rangle \,=\,&\\ \delta_{M0}\,(-i)^{2n_H+l_H}\sqrt{\frac{4}{\hbar\bar\omega_0}\sqrt{\frac{2\epsilon}{\pi\hbar\bar\omega_0}}}&\\ \cdot\int \mathrm{d}k k^2\; F^{{\rm pro},\,\tau}_{[lj,n_Hl_Hj_H]I0}(k,q)\,g^\epsilon_{\tau lj}(k)\,,&\end{aligned} \tag{2.27}$$

where now

$$\hbar\bar\omega_0 \equiv \hbar\omega_0\,\frac{b^2}{\bar b^2}\,. \tag{2.28}$$

Note that even in the "normal" expression (2.26) here the reduced mass enters, since the Woods-Saxon differential equation describes the relative motion of a nucleon with respect to the $(A-1)$-nucleon system. Obviously, for the corrected spectral-function approach (2.28) instead of (2.26) has to be used in eq. (2.25).

Now the target ground state is localized. Hence, in all matrix elements occuring in (2.25) and (2.27) the partial waves will give a non-vanishing contribution only within a finite interval in ordinary space, say $0 \le r \le R$. In this finite interval we can expand the regular solution of the Woods-Saxon differential equation for each energy ϵ and partial wave τlj in terms of Bessel functions at a finite (equidistant) grid of momenta. We write

$$\frac{v^\epsilon_{\tau lj}(r)}{r} \,=\, \sum_{i=1}^{N} j_l(k_i r)\,g_i(\epsilon\tau lj)\,. \tag{2.29}$$

Integration over the radial coordinate in the chosen finite interval yields then

$$g_i(\epsilon\tau lj) \,=\, \sum_{j=1}^{N}\left(M_l^{-1}\right)_{ij}\int\limits_0^R \mathrm{d}r\, r\, j_l(k_j r)\,v^\epsilon_{\tau lj}(r)\,, \tag{2.30}$$

where the inverse of the matrix

$$(M_l)_{ij} \,\equiv\, \int\limits_0^R \mathrm{d}r\, r^2\, j_l(k_i r)\, j_l(k_j r) \tag{2.31}$$

is needed because in the chosen finite interval the integration does not yield a Dirac delta-function in the momenta. The integrals in (2.25) and (2.27) can now be replaced by finite sums

$$\int \mathrm{d}k k^2\; F(k)\,g^\epsilon_{\tau lj}(k) \,=\, \sum_{i=1}^{N} F(k_i)\,g_i(\epsilon\tau lj)\,. \tag{2.32}$$

Finally, the longitudinal response functions are given by

$$R_L^{\rm nor}(\omega,\,q) \,=\, \sum_{\tau lj n_H l_H j_H I} |\langle C_\tau(\omega)\,[lj,n_Hl_Hj_H]I0|\,\hat\rho^{\rm nor}|\,\rangle|^2 \tag{2.33}$$

in the normal approach and

$$R_L^{\rm pro}(\omega,\,q) = \sum_{\tau lj n_H l_H j_H I} |\langle C_\tau(\omega);\,[lj,n_Hl_Hj_H]I0;\,(0)|\,\hat\rho^{\rm inv}|\,\rangle|^2 \tag{2.34}$$

in the Galilei-invariant approach, respectively. If only a particular hole state is to be considered, obviously the summation over $n_Hl_Hj_H$ and τ in these expressions has to be skipped.

Left to be evaluated are now the form factor functions F occuring in (2.25) and (2.27), respectively. For the $H = 0s$ holes in ^{4}He we obtain in the normal approximation

$$\begin{aligned}F^{{\rm nor},\,\tau}_{[lj,0s_{1/2}]I0}(k,q) \,=\,&\delta_{Il}(-)^{l+j-1/2}\sqrt{2(2j+1)}\\ \cdot\left(j\,\frac{1}{2}\,l|\frac{1}{2}-\frac{1}{2}0\right)&\left\{\exp\left[-\frac{\kappa^2+\lambda^2}{2}\right]\,J_l(\kappa\lambda)\,f_\tau\right.\\ \left.+\,\delta_{l0}\exp\left[-\frac{\kappa^2}{2}-\frac{\lambda^2}{4}\right]\,(2[f_\tau+f_{-\tau}]-f_\tau)\right\}&,\end{aligned} \tag{2.35}$$

while the Galilei-invariant result is

$$F^{\mathrm{pro},\,\tau}_{[lj,0s_{1/2}]I0}(k,q) \;=\; \delta_{Il}(-)^{l+j-1/2}\sqrt{2(2j+1)}$$
$$\cdot\left(j\,\frac{1}{2}\,l|\frac{1}{2}-\frac{1}{2}0\right)\left\{\exp\left[-\frac{\bar\kappa^2+\bar\lambda^2}{2}\right]J_l(\bar\kappa\bar\lambda)\,f_\tau\right.$$
$$+\exp\left[-\frac{\bar\kappa^2}{2}-\frac{10}{9}\cdot\frac{\bar\lambda^2}{4}\right](-)^l$$
$$\left.\cdot\,(2[f_\tau+f_{-\tau}]-f_\tau)\,J_l\left(\frac{\bar\kappa\bar\lambda}{3}\right)\right\}. \qquad (2.36)$$

In these expressions $J_l(x)$ are the so-called modified spherical Bessel functions of the first kind which are usually denoted by $\sqrt{\pi/2/x}\,I_{l+1/2}(x)$. Note that the second term of (2.35) contributes only for angular momentum $l=0$, while in the Galilei-invariant expression (2.36) the second term contributes for arbitrary angular momenta.

For the $H=0s$ holes in ^{16}O the normal prescription yields

$$F^{\mathrm{nor},\,\tau}_{[lj,0s_{1/2}]I0}(k,q) \;=\; \delta_{Il}(-)^{l+j-1/2}\sqrt{2(2j+1)}$$
$$\cdot\left(j\,\frac{1}{2}\,l|\frac{1}{2}-\frac{1}{2}0\right)\left\{\exp\left[-\frac{\kappa^2+\lambda^2}{2}\right]J_l(\kappa\lambda)\,f_\tau\right.$$
$$+\exp\left[-\frac{\kappa^2}{2}-\frac{\lambda^2}{4}\right]\left[8[f_\tau+f_{-\tau}]\left[1-\frac{\lambda^2}{8}\right]\delta_{l0}\right.$$
$$\left.\left.-\,f_\tau\left(\delta_{l0}+\frac{1}{3}\kappa\lambda\,\delta_{l1}\right)\right]\right\}, \qquad (2.37)$$

while respecting Galilei-invariance one obtains

$$F^{\mathrm{pro},\,\tau}_{[lj,0s_{1/2}]I0}(k,q) \;=\; \delta_{Il}(-)^{l+j-1/2}\sqrt{2(2j+1)}$$
$$\cdot\left(j\,\frac{1}{2}\,l|\frac{1}{2}-\frac{1}{2}0\right)\cdot\sqrt{\frac{4}{5}}\left\{\exp\left[-\frac{\bar\kappa^2+\bar\lambda^2}{2}\right]J_l(\bar\kappa\bar\lambda)\,f_\tau\right.$$
$$+\exp\left[-\frac{\bar\kappa^2}{2}-\frac{226}{225}\cdot\frac{\bar\lambda^2}{4}\right](-)^l\left[8[f_\tau+f_{-\tau}]\right.$$
$$\cdot\left[1-\frac{2}{15}\bar\lambda^2\right]\left(\left[1+\frac{2}{675}\bar\lambda^2\right]J_l\left(\frac{\bar\kappa\bar\lambda}{15}\right)\right.$$
$$\left.-\,\frac{4}{45}\bar\kappa\bar\lambda\left[\frac{l}{2l+1}J_{l-1}\left(\frac{\bar\kappa\bar\lambda}{15}\right)+\frac{l+1}{2l+1}J_{l+1}\left(\frac{\bar\kappa\bar\lambda}{15}\right)\right]\right)$$
$$-\,f_\tau\left(\left[1+\frac{32}{675}\bar\lambda^2-\frac{16}{10125}\bar\lambda^4\right]J_l\left(\frac{\bar\kappa\bar\lambda}{15}\right)\right.$$
$$-\,\frac{64}{45}\bar\kappa\bar\lambda\left[1-\frac{1}{30}\bar\lambda^2\right]\left[\frac{l}{2l+1}J_{l-1}\left(\frac{\bar\kappa\bar\lambda}{15}\right)\right.$$
$$\left.\left.\left.\left.+\,\frac{l+1}{2l+1}J_{l+1}\left(\frac{\bar\kappa\bar\lambda}{15}\right)\right]\right)\right]\right\}. \qquad (2.38)$$

Again, in the projected expression (2.38) the second term contributes for all angular momenta, while the second term of the normal expression (2.37) is limited to the angular momenta of the occupied s- and p-states. Furthermore, as compared to the normal expression (2.37) in the Galilei-invariant result (2.38) the square root of the spectroscopic factor (2.20) occurs as an overall factor.

For the $0p$ holes in ^{16}O the normal result is

$$F^{\mathrm{nor},\,\tau}_{[lj,0p_{j_H}]I0}(k,q) \;=\; \delta_{Il\pm1}(-)^{I+j-1/2}$$
$$\cdot\sqrt{(2j_H+1)(2j+1)}\left(jj_HI|\frac{1}{2}-\frac{1}{2}0\right)\cdot\sqrt{\frac{2}{3}}$$
$$\cdot\left\{\exp\left[-\frac{\kappa^2+\lambda^2}{2}\right]\,[\kappa J_I(\kappa\lambda)\,-\,\lambda J_l(\kappa\lambda)]\,f_\tau\right.$$
$$+\exp\left[-\frac{\kappa^2}{2}-\frac{\lambda^2}{4}\right]\left[8[f_\tau+f_{-\tau}]\left[1-\frac{\lambda^2}{8}\right]\kappa\delta_{I0}\right.$$
$$\left.\left.-\,f_\tau\left(\kappa\delta_{I0}-\frac{1}{6}\kappa\lambda^2\,\delta_{l1}-\frac{1}{2}\lambda\,\delta_{l0}\right)\right]\right\}, \qquad (2.39)$$

while Galilei invariance requires

$$F^{\mathrm{pro},\,\tau}_{[lj,0p_{j_H}]I0}(k,q) = \delta_{Il\pm1}(-)^{I+j-1/2}$$
$$\cdot\sqrt{(2j_H+1)(2j+1)}\left(jj_HI|\frac{1}{2}-\frac{1}{2}0\right)\cdot\sqrt{\frac{16}{15}}\cdot\sqrt{\frac{2}{3}}$$
$$\cdot\left\{\exp\left[-\frac{\bar\kappa^2+\bar\lambda^2}{2}\right]\,\left[\bar\kappa J_I(\bar\kappa\bar\lambda)\,-\,\bar\lambda J_l(\bar\kappa\bar\lambda)\right]\,f_\tau\right.$$
$$+\exp\left[-\frac{\bar\kappa^2}{2}-\frac{226}{225}\cdot\frac{\bar\lambda^2}{4}\right](-)^I\left[8[f_\tau+f_{-\tau}]\left[1-\frac{2}{15}\bar\lambda^2\right]\right.$$
$$\cdot\left[\bar\kappa\,J_I\left(\frac{\bar\kappa\bar\lambda}{15}\right)\,-\,\frac{1}{30}\bar\lambda\,J_l\left(\frac{\bar\kappa\bar\lambda}{15}\right)\right]$$
$$-\,f_\tau\left(\bar\kappa\,J_I\left(\frac{\bar\kappa\bar\lambda}{15}\right)\,+\,\frac{7}{15}\bar\lambda\left[1+\frac{4}{105}\bar\lambda^2\right]\,J_l\left(\frac{\bar\kappa\bar\lambda}{15}\right)\right.$$
$$\left.\left.\left.\left.-\,\frac{8}{15}\bar\kappa\bar\lambda^2\left[\frac{l}{2l+1}J_{l-1}\left(\frac{\bar\kappa\bar\lambda}{15}\right)+\frac{l+1}{2l+1}J_{l+1}\left(\frac{\bar\kappa\bar\lambda}{15}\right)\right]\right)\right]\right\}, \qquad (2.40)$$

which again has the square root of the spectroscopic factor from (2.20) as overall factor.

Finally we come to the case of ^{40}Ca. For the $H=0s$ holes one obtains in the conventional approach

$$F^{\mathrm{nor},\,\tau}_{[lj,0s_{1/2}]I0}(k,q) \;=\; \delta_{Il}(-)^{l+j-1/2}\sqrt{2(2j+1)}$$
$$\cdot\left(j\,\frac{1}{2}\,l|\frac{1}{2}-\frac{1}{2}0\right)\left\{\exp\left[-\frac{\kappa^2+\lambda^2}{2}\right]\,J_l(\kappa\lambda)\,f_\tau\right.$$
$$+\exp\left[-\frac{\kappa^2}{2}-\frac{\lambda^2}{4}\right]\left[20[f_\tau+f_{-\tau}]\left[1-\frac{\lambda^2}{4}+\frac{\lambda^4}{80}\right]\delta_{l0}\right.$$
$$\left.\left.-\,f_\tau\left(\left[1-\frac{\lambda^2}{4}+\frac{\kappa^2\lambda^2}{6}\right]\delta_{l0}+\frac{\kappa\lambda}{3}\,\delta_{l1}+\frac{\kappa^2\lambda^2}{15}\,\delta_{l2}\right)\right]\right\}, \qquad (2.41)$$

while with projection

$$
\begin{aligned}
F^{\mathrm{pro},\tau}_{[lj,0\tilde{s}_{1/2}]I0}(k,q) \;=\; & \delta_{Il}(-)^{l+j-1/2}\sqrt{2(2j+1)} \\
& \cdot \left(j\,\frac{1}{2}\,l|\frac{1}{2}-\frac{1}{2}0\right)\cdot\sqrt{\frac{1410}{1521}}\Bigg\{\exp\left[-\frac{\bar{\kappa}^2+\bar{\lambda}^2}{2}\right]\,J_l(\bar{\kappa}\bar{\lambda})\,f_\tau \\
& +\exp\left[-\frac{\bar{\kappa}^2}{2}-\frac{1522}{1521}\cdot\frac{\bar{\lambda}^2}{4}\right](-)^l\Bigg[20[f_\tau+f_{-\tau}] \\
& \cdot\left[1-\frac{10}{39}\bar{\lambda}^2+\frac{20}{1521}\bar{\lambda}^4\right]\Bigg\{\Bigg[1+\frac{10}{71487}\bar{\lambda}^2 \\
& +\frac{20}{326195181}\bar{\lambda}^4\Bigg]J_l\left(\frac{\bar{\kappa}\bar{\lambda}}{39}\right)-\frac{140}{5499}\bar{\kappa}\bar{\lambda}\left[1+\frac{4}{10647}\bar{\lambda}^2\right] \\
& \cdot\left[\frac{l}{2l+1}J_{l-1}\left(\frac{\bar{\kappa}\bar{\lambda}}{39}\right)+\frac{l+1}{2l+1}J_{l+1}\left(\frac{\bar{\kappa}\bar{\lambda}}{39}\right)\right] \\
& +\frac{80}{214461}\bar{\kappa}^2\bar{\lambda}^2\Bigg[\frac{2l(l+1)-1}{(2l-1)(2l+3)}J_l\left(\frac{\bar{\kappa}\bar{\lambda}}{39}\right) \\
& +\frac{l(l-1)}{(2l+1)(2l-1)}J_{l-2}\left(\frac{\bar{\kappa}\bar{\lambda}}{39}\right) \\
& +\frac{(l+1)(l+2)}{(2l+1)(2l+3)}J_{l+2}\left(\frac{\bar{\kappa}\bar{\lambda}}{39}\right)\Bigg]\Bigg\} \\
& -f_\tau\Bigg\{\Bigg[1-\frac{6800}{23829}\bar{\lambda}^2+\frac{1319000}{326195181}\bar{\lambda}^4 \\
& -\frac{344000}{12721612059}\bar{\lambda}^6+\frac{4000}{496142870301}\bar{\lambda}^8\Bigg]J_l\left(\frac{\bar{\kappa}\bar{\lambda}}{39}\right) \\
& -\frac{5600}{5499}\bar{\kappa}\bar{\lambda}\left[1-\frac{359}{21294}\bar{\lambda}^2-\frac{121}{415233}\bar{\lambda}^4+\frac{20}{16194087}\bar{\lambda}^6\right] \\
& \cdot\left[\frac{l}{2l+1}J_{l-1}\left(\frac{\bar{\kappa}\bar{\lambda}}{39}\right)+\frac{l+1}{2l+1}J_{l+1}\left(\frac{\bar{\kappa}\bar{\lambda}}{39}\right)\right] \\
& +\frac{128000}{214461}\bar{\kappa}^2\bar{\lambda}^2\left[1-\frac{41}{3120}\bar{\lambda}^2+\frac{1}{12168}\bar{\lambda}^4\right] \\
& \cdot\left[\frac{2l(l+1)-1}{(2l-1)(2l+3)}J_l\left(\frac{\bar{\kappa}\bar{\lambda}}{39}\right)+\frac{l(l-1)}{(2l+1)(2l-1)}J_{l-2}\left(\frac{\bar{\kappa}\bar{\lambda}}{39}\right)\right. \\
& \left.+\frac{(l+1)(l+2)}{(2l+1)(2l+3)}J_{l+2}\left(\frac{\bar{\kappa}\bar{\lambda}}{39}\right)\right]\Bigg]\Bigg]\Bigg\}. \qquad (2.42)
\end{aligned}
$$

For the $H=0p$ hole in ^{40}Ca the normal prescription yields

$$
\begin{aligned}
F^{\mathrm{nor},\tau}_{[lj,0p_{j_H}]I0}(k,q) \;=\; & \delta_{Il\pm1}(-)^{I+j-1/2}\sqrt{(2j_H+1)(2j+1)} \\
& \cdot\left(jj_HI|\frac{1}{2}-\frac{1}{2}0\right)\cdot\sqrt{\frac{2}{3}}\Bigg\{\exp\left[-\frac{\kappa^2+\lambda^2}{2}\right] \\
& \cdot\left[\kappa J_I(\kappa\lambda)\;-\;\lambda J_l(\kappa\lambda)\right]\,f_\tau\,+\exp\left[-\frac{\kappa^2}{2}-\frac{\lambda^2}{4}\right] \\
& \cdot\left[20[f_\tau+f_{-\tau}]\left[1-\frac{\lambda^2}{4}+\frac{\lambda^4}{80}\right]\kappa\delta_{I0}\right. \\
& -f_\tau\Bigg(\kappa\delta_{I0}+\frac{\kappa^2\lambda}{3}\,\delta_{I1}-\lambda\left[1-\frac{\lambda^2}{8}+\frac{\kappa^2\lambda^2}{12}\right]\,\delta_{l0} \\
& \left.-\frac{\kappa\lambda^2}{6}\,\delta_{l1}-\frac{\kappa^2\lambda^3}{30}\,\delta_{l2}\Bigg)\right]\Bigg\}, \qquad (2.43)
\end{aligned}
$$

while Galilei invariance requires

$$
\begin{aligned}
F^{\mathrm{pro},\tau}_{[lj,0p_{j_H}]I0}(k,q) \;=\; & \delta_{Il\pm1}(-)^{I+j-1/2}\sqrt{(2j_H+1)(2j+1)} \\
& \cdot\left(jj_HI|\frac{1}{2}-\frac{1}{2}0\right)\cdot\sqrt{\frac{1400}{1521}}\cdot\sqrt{\frac{2}{3}}\Bigg\{\exp\left[-\frac{\bar{\kappa}^2+\bar{\lambda}^2}{2}\right] \\
& \cdot\left[\bar{\kappa}J_I(\bar{\kappa}\bar{\lambda})\;-\;\bar{\lambda}J_l(\bar{\kappa}\bar{\lambda})\right]\,f_\tau+\exp\left[-\frac{\bar{\kappa}^2}{2}-\frac{1522}{1521}\cdot\frac{\bar{\lambda}^2}{4}\right] \\
& \cdot(-)^I\Bigg[20[f_\tau+f_{-\tau}]\left[1-\frac{10}{39}\bar{\lambda}^2+\frac{20}{1521}\bar{\lambda}^4\right]\cdot \\
& \cdot\Bigg\{\bar{\kappa}\left[1+\frac{4}{10647}\bar{\lambda}^2\right]\,J_I\left(\frac{\bar{\kappa}\bar{\lambda}}{39}\right)+\frac{1}{546}\bar{\lambda}\left[1-\frac{4}{1521}\bar{\lambda}^2\right] \\
& \cdot J_l\left(\frac{\bar{\kappa}\bar{\lambda}}{39}\right)\;+\;\frac{4}{10647}\bar{\kappa}\bar{\lambda}^2\left[\frac{l}{2l+1}J_{l-1}\left(\frac{\bar{\kappa}\bar{\lambda}}{39}\right)\right. \\
& \left.+\frac{l+1}{2l+1}J_{l+1}\left(\frac{\bar{\kappa}\bar{\lambda}}{39}\right)\right]\;-\;\frac{8}{273}\bar{\kappa}^2\bar{\lambda}\left[\frac{I}{2I+1}J_{I-1}\left(\frac{\bar{\kappa}\bar{\lambda}}{39}\right)\right. \\
& \left.+\frac{I+1}{2I+1}J_{I+1}\left(\frac{\bar{\kappa}\bar{\lambda}}{39}\right)\right]\Bigg\}\;-\;f_\tau\Bigg\{\bar{\kappa}\left[1+\frac{160}{10647}\bar{\lambda}^2\right. \\
& \left.-\frac{80}{415233}\bar{\lambda}^4\right]\,J_I\left(\frac{\bar{\kappa}\bar{\lambda}}{39}\right)\;+\;\frac{293}{273}\bar{\lambda}\left[1-\frac{64430}{445653}\bar{\lambda}^2\right. \\
& \left.+\frac{32060}{17380467}\bar{\lambda}^4-\frac{400}{677838213}\bar{\lambda}^6\right]\,J_l\left(\frac{\bar{\kappa}\bar{\lambda}}{39}\right) \\
& -\frac{5300}{10647}\bar{\kappa}\bar{\lambda}^2\left[1+\frac{56}{3445}\bar{\lambda}^2\;-\;\frac{16}{80613}\bar{\lambda}^4\right] \\
& \cdot\left[\frac{l}{2l+1}J_{l-1}\left(\frac{\bar{\kappa}\bar{\lambda}}{39}\right)\;+\;\frac{l+1}{2l+1}J_{l+1}\left(\frac{\bar{\kappa}\bar{\lambda}}{39}\right)\right] \\
& +\frac{3280}{10647}\bar{\kappa}^2\bar{\lambda}^3\left[1-\frac{20}{1599}\bar{\lambda}^2\right]\left[\frac{2l(l+1)-1}{(2l-1)(2l+3)}J_l\left(\frac{\bar{\kappa}\bar{\lambda}}{39}\right)\right. \\
& +\frac{l(l-1)}{(2l+1)(2l-1)}J_{l-2}\left(\frac{\bar{\kappa}\bar{\lambda}}{39}\right)+\frac{(l+1)(l+2)}{(2l+1)(2l+3)} \\
& \left.\cdot J_{l+2}\left(\frac{\bar{\kappa}\bar{\lambda}}{39}\right)\right]\;-\;\frac{320}{273}\bar{\kappa}^2\bar{\lambda}\left[1-\frac{1}{78}\bar{\lambda}^2\right]\left[\frac{I}{2I+1}\right. \\
& \left.\cdot J_{I-1}\left(\frac{\bar{\kappa}\bar{\lambda}}{39}\right)\;+\;\frac{I+1}{2I+1}J_{I+1}\left(\frac{\bar{\kappa}\bar{\lambda}}{39}\right)\right]\Bigg\}\Bigg]\Bigg\}. \qquad (2.44)
\end{aligned}
$$

For the $H = 1s$ holes we get

$$
\begin{aligned}
&F^{\mathrm{nor},\tau}_{[lj,1s_{1/2}]I0}(k,q) \;=\; \delta_{Il}(-)^{l+j-1/2}\sqrt{2(2j+1)} \\
&\cdot\left(j\,\frac{1}{2}\,l|\frac{1}{2}-\frac{1}{2}0\right)\cdot\sqrt{\frac{3}{2}}\Bigg\{\exp\left[-\frac{\kappa^2+\lambda^2}{2}\right]\,f_\tau \\
&\cdot\Bigg(\left[1-\frac{2}{3}\kappa^2-\frac{2}{3}\lambda^2\right]J_l(\kappa\lambda)\;+\;\frac{4}{3}\kappa\lambda\left[\frac{l}{2l+1}J_{l-1}(\kappa\lambda)\right. \\
&\left.+\,\frac{l+1}{2l+1}J_{l+1}(\kappa\lambda)\right]\Bigg)\;+\;\exp\left[-\frac{\kappa^2}{2}-\frac{\lambda^2}{4}\right] \\
&\cdot\left[20[f_\tau+f_{-\tau}]\left[1-\frac{\lambda^2}{4}+\frac{\lambda^4}{80}\right]\left[1-\frac{2}{3}\kappa^2\right]\delta_{l0}\right. \\
&-f_\tau\Bigg(\left[1-\frac{2}{3}\kappa^2-\frac{\lambda^2}{2}+\frac{\lambda^4}{24}+\frac{2}{9}\kappa^2\lambda^2-\frac{1}{36}\kappa^2\lambda^4\right]\delta_{l0} \\
&\left.+\frac{2}{9}\kappa\lambda\left[1-\frac{\lambda^2}{4}\right]\delta_{l1}+\frac{4}{45}\kappa^2\lambda^2\left[1-\frac{\lambda^2}{8}\right]\delta_{l2}\Bigg)\right]\Bigg\} \qquad (2.45)
\end{aligned}
$$

and

$$
\begin{aligned}
&F^{\mathrm{pro},\tau}_{[lj,1s_{1/2}]I0}(k,q) \;=\; \delta_{Il}(-)^{l+j-1/2}\sqrt{2(2j+1)} \\
&\cdot\left(j\,\frac{1}{2}\,l|\frac{1}{2}-\frac{1}{2}0\right)\cdot\sqrt{\frac{1600}{1521}}\cdot\sqrt{\frac{3}{2}}\Bigg\{\exp\left[-\frac{\bar\kappa^2+\bar\lambda^2}{2}\right]\,f_\tau \\
&\cdot\Bigg(\left[1-\frac{2}{3}\bar\kappa^2-\frac{2}{3}\bar\lambda^2\right]J_l(\bar\kappa\bar\lambda)\;+\;\frac{4}{3}\bar\kappa\bar\lambda\left[\frac{l}{2l+1}J_{l-1}(\bar\kappa\bar\lambda)\right. \\
&\left.+\,\frac{l+1}{2l+1}J_{l+1}(\bar\kappa\bar\lambda)\right]\Bigg)\;+\;\exp\left[-\frac{\bar\kappa^2}{2}-\frac{1522}{1521}\cdot\frac{\bar\lambda^2}{4}\right](-)^l \\
&\cdot\left[20[f_\tau+f_{-\tau}]\left[1-\frac{10}{39}\bar\lambda^2+\frac{20}{1521}\bar\lambda^4\right]\right. \\
&\cdot\Bigg\{\left[1-\frac{2}{3}\bar\kappa^2-\frac{1}{9126}\bar\lambda^2\right]J_l\left(\frac{\bar\kappa\bar\lambda}{39}\right) \\
&+\,\frac{2}{117}\bar\kappa\bar\lambda\left[\frac{l}{2l+1}J_{l-1}\left(\frac{\bar\kappa\bar\lambda}{39}\right)+\frac{l+1}{2l+1}J_{l+1}\left(\frac{\bar\kappa\bar\lambda}{39}\right)\right]\Bigg\} \\
&-f_\tau\Bigg\{\left[1-\frac{2}{3}\bar\kappa^2-\frac{2282}{4563}\bar\lambda^2+\frac{7430}{177957}\bar\lambda^4-\frac{100}{6940323}\bar\lambda^6\right] \\
&\cdot J_l\left(\frac{\bar\kappa\bar\lambda}{39}\right)\;-\;\frac{76}{117}\bar\kappa\bar\lambda\left[1-\frac{175}{741}\bar\lambda^2-\frac{100}{28899}\bar\lambda^4\right] \\
&\cdot\left[\frac{l}{2l+1}J_{l-1}\left(\frac{\bar\kappa\bar\lambda}{39}\right)+\frac{l+1}{2l+1}J_{l+1}\left(\frac{\bar\kappa\bar\lambda}{39}\right)\right] \\
&+\,\frac{80}{117}\bar\kappa^2\bar\lambda^2\left[1-\frac{5}{39}\bar\lambda^2\right]\left[\frac{2l(l+1)-1}{(2l-1)(2l+3)}J_l\left(\frac{\bar\kappa\bar\lambda}{39}\right)\right. \\
&+\,\frac{l(l-1)}{(2l+1)(2l-1)}J_{l-2}\left(\frac{\bar\kappa\bar\lambda}{39}\right) \\
&\left.\left.\left.+\,\frac{(l+1)(l+2)}{(2l+1)(2l+3)}J_{l+2}\left(\frac{\bar\kappa\bar\lambda}{39}\right)\right]\right]\Bigg\}\Bigg\}. \qquad (2.46)
\end{aligned}
$$

For the $H = 0d$ holes, finally, we have

$$
\begin{aligned}
&F^{\mathrm{nor},\tau}_{[lj,0d_{j_H}]I0}(k,q) \;=\; (-)^{I+j-1/2}\sqrt{(2j_H+1)(2j+1)} \\
&\cdot\left(jj_HI|\frac{1}{2}-\frac{1}{2}0\right)\cdot\frac{2}{\sqrt{15}}\Bigg\{\exp\left[-\frac{\kappa^2+\lambda^2}{2}\right]\,f_\tau \\
&\cdot\Bigg(\kappa^2\,J_I(\kappa\lambda)+\lambda^2\,J_l(\kappa\lambda)\;-\;2\kappa\lambda \\
&\cdot\left[\frac{(l+2)(l+3)-I(I+1)}{4(2l+1)}J_{l-1}(\kappa\lambda)\right. \\
&\left.+\,\frac{I(I+1)-(l-1)(l-2)}{4(2l+1)}J_{l+1}(\kappa\lambda)\right]\Bigg) \\
&+\,\exp\left[-\frac{\kappa^2}{2}-\frac{\lambda^2}{4}\right]\left[20[f_\tau+f_{-\tau}]\left[1-\frac{\lambda^2}{4}+\frac{\lambda^4}{80}\right]\right. \\
&\cdot\kappa^2\delta_{I0}\;-\;f_\tau\Bigg(\kappa^2\,\delta_{I0}+\frac{3}{4}\lambda^2\left[1-\frac{\lambda^2}{12}+\frac{\kappa^2\lambda^2}{18}\right]\delta_{l0} \\
&\left.+\,\frac{\kappa\lambda^3}{12}\,\delta_{l1}-\frac{5}{6}\kappa\lambda\,\delta_{I1}\delta_{l1}+\frac{\kappa^2\lambda^4}{60}\,\delta_{l2}\Bigg)\right]\Bigg\} \qquad (2.47)
\end{aligned}
$$

and

$$
\begin{aligned}
&F^{\mathrm{pro},\tau}_{[lj,0d_{j_H}]I0}(k,q) \;=\; (-)^{I+j-1/2}\sqrt{(2j_H+1)(2j+1)} \\
&\cdot\left(jj_HI|\frac{1}{2}-\frac{1}{2}0\right)\cdot\sqrt{\frac{1600}{1521}}\cdot\frac{2}{\sqrt{15}}\Bigg\{\exp\left[-\frac{\bar\kappa^2+\bar\lambda^2}{2}\right]\,f_\tau \\
&\cdot\Bigg(\bar\kappa^2J_I(\bar\kappa\bar\lambda)+\bar\lambda^2J_l(\bar\kappa\bar\lambda)-2\bar\kappa\bar\lambda\left[\frac{(l+2)(l+3)-I(I+1)}{4(2l+1)}\right. \\
&\left.\cdot\,J_{l-1}(\bar\kappa\bar\lambda)+\frac{I(I+1)-(l-1)(l-2)}{4(2l+1)}J_{l+1}(\bar\kappa\bar\lambda)\right]\Bigg) \\
&+\,\exp\left[-\frac{\bar\kappa^2}{2}-\frac{1522}{1521}\cdot\frac{\bar\lambda^2}{4}\right](-)^I\left[20[f_\tau+f_{-\tau}]\right. \\
&\cdot\left[1-\frac{10}{39}\bar\lambda^2+\frac{20}{1521}\bar\lambda^4\right]\Bigg\{\bar\kappa^2\,J_I\left(\frac{\bar\kappa\bar\lambda}{39}\right)+\frac{1}{6084}\bar\lambda^2 \\
&\cdot J_l\left(\frac{\bar\kappa\bar\lambda}{39}\right)\;-\;\frac{\bar\kappa\bar\lambda}{39}\left[\frac{(l+2)(l+3)-I(I+1)}{4(2l+1)}J_{l-1}\left(\frac{\bar\kappa\bar\lambda}{39}\right)\right. \\
&\left.+\,\frac{I(I+1)-(l-1)(l-2)}{4(2l+1)}J_{l+1}\left(\frac{\bar\kappa\bar\lambda}{39}\right)\right]\Bigg\} \\
&-f_\tau\Bigg(\bar\kappa^2\,J_I\left(\frac{\bar\kappa\bar\lambda}{39}\right)\;+\;\frac{1141}{1521}\bar\lambda^2\left[1-\frac{3715}{44499}\bar\lambda^2\right. \\
&\left.+\,\frac{50}{1735461}\bar\lambda^4\right]J_l\left(\frac{\bar\kappa\bar\lambda}{39}\right)\;-\;\frac{38}{39}\bar\kappa\bar\lambda\left[1+\frac{10}{741}\bar\lambda^2\right] \\
&\cdot\left[\frac{(l+2)(l+3)-I(I+1)}{4(2l+1)}J_{l-1}\left(\frac{\bar\kappa\bar\lambda}{39}\right)\right.
\end{aligned}
$$

$$+\frac{I(I+1)-(l-1)(l-2)}{4(2l+1)}J_{l+1}\left(\frac{\bar{\kappa}\bar{\lambda}}{39}\right)\Bigg]$$
$$-\frac{370}{1521}\bar{\kappa}\bar{\lambda}^3\left[1+\frac{20}{1433}\bar{\lambda}^2\right]\left[\frac{l}{2l+1}J_{l-1}\left(\frac{\bar{\kappa}\bar{\lambda}}{39}\right)\right.$$
$$\left.+\frac{l+1}{2l+1}J_{l+1}\left(\frac{\bar{\kappa}\bar{\lambda}}{39}\right)\right]+\frac{200}{1521}\bar{\kappa}^2\bar{\lambda}^4\left[\frac{2l(l+1)-1}{(2l-1)(2l+3)}\right.$$
$$\cdot J_l\left(\frac{\bar{\kappa}\bar{\lambda}}{39}\right)+\frac{l(l-1)}{(2l-1)(2l+1)}J_{l-2}\left(\frac{\bar{\kappa}\bar{\lambda}}{39}\right)$$
$$\left.+\frac{(l+1)(l+2)}{(2l+1)(2l+3)}J_{l+2}\left(\frac{\bar{\kappa}\bar{\lambda}}{39}\right)\right]$$
$$-\frac{40}{39}\bar{\kappa}^2\bar{\lambda}^2\left[\frac{(l-1)[(l+2)(l+3)-I(I+1)]}{4(2l-1)(2l+1)}J_{l-2}\right.$$
$$\cdot\left(\frac{\bar{\kappa}\bar{\lambda}}{39}\right)+\frac{(l+2)[I(I+1)-(l-1)(l-2)]}{4(2l+3)(2l+1)}J_{l+2}\left(\frac{\bar{\kappa}\bar{\lambda}}{39}\right)$$
$$\left.+\frac{9l(l+1)-2-I(I+1)}{4(2l-1)(2l+3)}J_l\left(\frac{\bar{\kappa}\bar{\lambda}}{39}\right)\right]\Bigg)\Bigg]\Bigg\}, \quad (2.48)$$

respectively.

Before starting with the numerical evaluation it is worthwhile to discuss the general structure of these results for a moment. First of all, the projected form factor functions differ by an overall factor, the square root of the spectroscopic factor, from the normal expressions. Because of (2.20) this means that the contributions of the holes in the last occupied shell will be enhanced those of the holes out of the lower shells quenched with respect to the normal results. Furthermore, in the projected expressions the momentum transfer is reduced by a factor $(A-1)/A$ with respect to the normal approach, while the wave vector of the outgoing nucleon is enhanced thus causing a faster fall-off of the projected matrix elements with transferred energy. Together this has the effect that the projected response functions will be peaked at smaller energy losses than the normal ones. Finally, as already mentioned, out of orthogonality reasons the second term in (2.10) will give only a very small contribution even though oscillator instead of Woods-Saxon wave functions are used for the bound states. For the second term of the projected approach this is not *a priori* true. Here, as can be seen from the form factor formulas, partial waves with arbitrary angular momenta and not only with the angular momenta of the bound states do contribute. The comparison with the above-mentioned corrected spectral-function approximation will, however, demonstrate, that even in the projected approach the effects of the second term (and hence the non-orthogonality effects, too) are almost negligible.

3 Results and discussion

Equations (2.33) and (2.34) have been evaluated for a total 3-momentum transfer of 500 MeV/c for the three nuclei ^{4}He, ^{16}O and ^{40}Ca. For the nucleon form factors (2.7) in all three cases the standard dipole parametrisation (2.8) has been taken. Furthermore, the calculations were repeated for $f_p = 1$ and $f_n = 0$ in eq. (2.7). This allows a comparison with the mathematical sum rules discussed in [2]. The quasi-elastic limit (*i.e.* large q) yielded there Z for the Coulomb sum rule in both the projected as well as the normal approach. For the most probable energy loss (essentially the first moment of the longitudinal response function) the COM-projected approach gave $q^2/2M_N$, while in the normal description this value has to be multiplied with $(1+1/A)$. Finally the widths of the longitudinal response functions (essentially the second moment) were proportional to the ground-state expectation value of the projected or normal kinetic energy, respectively.

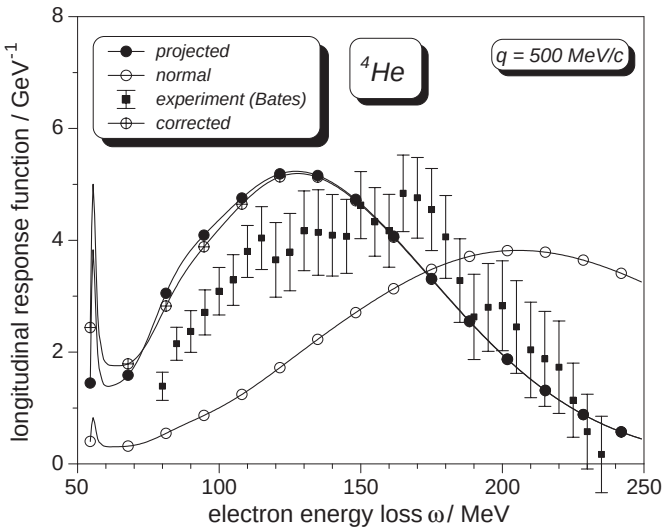

Fig. 1. The longitudinal response of ^{4}He to inelastic electron scattering at the 3-momentum transfer $q = 500$ MeV/c. The experimental data have been taken from Bates [6]. Open circles give the "normal" result (2.33), while full circles refer to the Galilei-invariant version (2.34) of our simple knock-out model. Finally, crossed circles stand for the spectral-function part of the normal description "corrected" by quenching the momentum transfer with a factor $(A-1)/A$ and using relative hole wave functions according to eqs. (2.21) and (2.22).

Let us start with ^{4}He. Here the Woods-Saxon parameters have been the following: the depth of the potential (2.4) was $U_0 = -57.23$ MeV, the spin-orbit term $U_{ls} = -5.00$ MeV, and for the surface thickness $a_0 = a_{ls} = 0.2$ fm have been taken. Furthermore, for the parametrisation (2.5) of the radii $r_0 = r_{ls} = r_C = 1.38672$ fm has been used. The optimisation of the oscillator length in order to get maximal overlap between the Woods-Saxon and the oscillator $0s$ bound state yielded here $b = 1.41613$ fm. The expansion (2.30) of the Woods-Saxon partial waves in terms of plane waves was performed with a cut-off $R = 10$ fm.

The results are displayed in fig. 1. The open circles refer to the normal approximation (2.33), the full ones to the Galilei-invariant result (2.34). Crossed open circles indicate the "corrected" result if for the normal approach only the spectral-function part is taken, however, modified

by eqs. (2.21-2.22), *i.e.*, the momentum transfer has been quenched by $A - 1/A = 3/4$ and instead of the bare nucleon mass the reduced mass $4M_N/3$ has been used. Furthermore, the experimental data from the Bates accelerator [6] are presented.

First of all, due to the restoration of Galilei invariance a tremendous shift of the peak position to lower-energy loss is observed. The maximum of the response function is shifted from 205.4 MeV to 126.8 MeV. In fact, without nuclear form factors, we obtain in the normal approximation for the Coulomb sum rule 1.995, for the most probable energy loss $\bar{\omega} = 211.0$ MeV and for the width of the distribution 70.5 MeV. On the other hand, the Galilei-invariant description yields 1.974 for the Coulomb sum rule, 136.6 MeV for $\bar{\omega}$ and only 45.9 MeV for the width. For the chosen momentum transfer $q^2/2M_N = 133.1$ MeV. Thus, the projected result is already rather near to the quasi-elastic limit. It is interesting to note that $133.1(1 + 1/4 + 1/3) = 211$. The $1/A$ factor was to be expected from the discussion of sum rules in the closure approximation in [2], the additional $1/(A-1)$ comes from the neglection of the recoil in the normal description of the scattering states.

Second, one observes that the experimental data are almost right in the middle between the normal and the projected response functions. Thus, if one makes some kind of "recoil correction" in the normal approach but neglects the projection into the COM rest frame, one can reproduce the right position of the experimental peak (see, *e.g.*, ref. [7]). This, however, is by chance. As we shall demonstrate in the next of the present series of papers, the difference of the Galilei-invariant uncorrelated result in fig. 1 and the experimental data can be accounted for entirely by conventional nucleon-nucleon correlations.

Last but not least, it can be seen from the figure that the corrected spectral-function approach is here an excellent approximation to the full COM-projected result. Thus the additional terms in (2.38) give indeed only a rather small contribution.

For ^{16}O and ^{40}Ca we took as Woods-Saxon parameters for protons and neutrons $a_0 = a_{ls} = 0.53$ fm and $r_0 = r_{ls} = 1.209$ fm. For the protons $U_0 = -55.81$ MeV, $U_{ls} = -6.675$ MeV, and $r_C = 1.25$ fm, while for the neutrons $U_0 = -55.50$ MeV and $U_{ls} = -6.675$ MeV. The upper limit for the expansion interval was here always $R = 14$ fm. For the optimized oscillator length parameter we obtained $b = 1.7$ fm and $b = 1.818$ fm for ^{16}O and ^{40}Ca, respectively.

Let us first discuss the case of ^{16}O. Using no form factors, we obtain in the normal approach 7.894 for the Coulomb sum rule, 157.4 MeV for the most probable energy loss and 56.4 MeV for the width, while the Galilei-invariant approach yields 7.888, 141.9 MeV and 51.9 MeV, respectively. As compared to the ^{4}He result we are here still further away from the quasi-elastic limit. This is also seen from the fact that $133.1(1+1/16+1/15)$ is only 150.3.

The results obtained with the standard parametrisation (2.8) of the nucleon form factors (2.7) are displayed in figs. 2 and 3, respectively. Figure 2 shows the total longitudinal reponse of ^{16}O as observed in inclusive scattering. Again the normal prescription, the full Galilei-invariant result and the corrected spectral-function approach are compared with each other. Also here due to the restoration of Galilei invariance a shift of the peak position to lower energy loss is observed though here as expected from the larger nucleon number the maximum is shifted only by 18.9 MeV from 167.4 MeV to 148.5 MeV. Again, the corrected spectral-function approach yields an excellent reproduction of the full Galilei-invariant result.

Figure 3 shows the decomposition of the total longitudinal response functions into the contributions from the various residual hole states. Since the contributions from

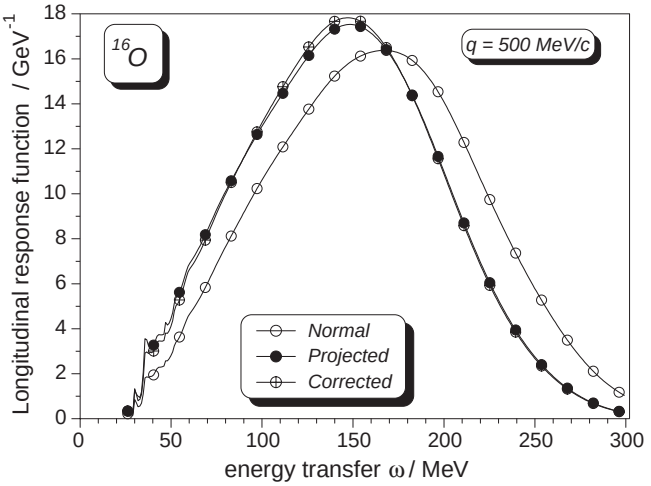

Fig. 2. Same as in fig. 1 but for the nucleus ^{16}O. Here no experimental data are available.

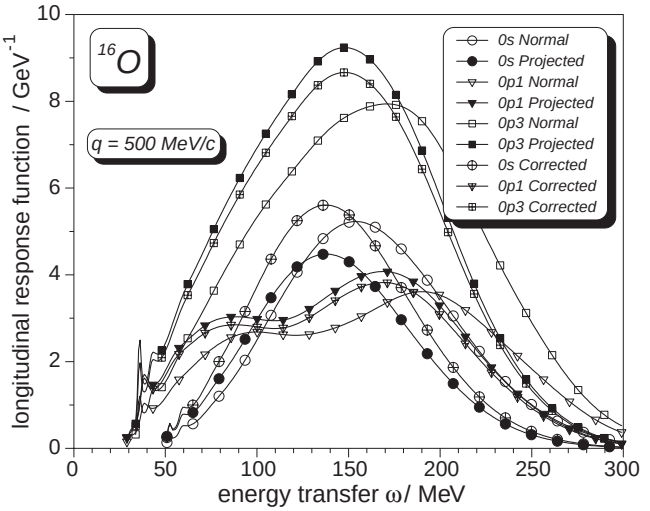

Fig. 3. The longitudinal response of ^{16}O to inelastic electron scattering at the 3-momentum transfer $q = 500$ MeV/c out of fig. 2 is decomposed into the various contributions from the different proton-hole states (the contributions of the neutron-hole states are almost negligible). Again open symbols refer to the "normal", full symbols to the "projected" and crossed symbols to the "corrected" results.

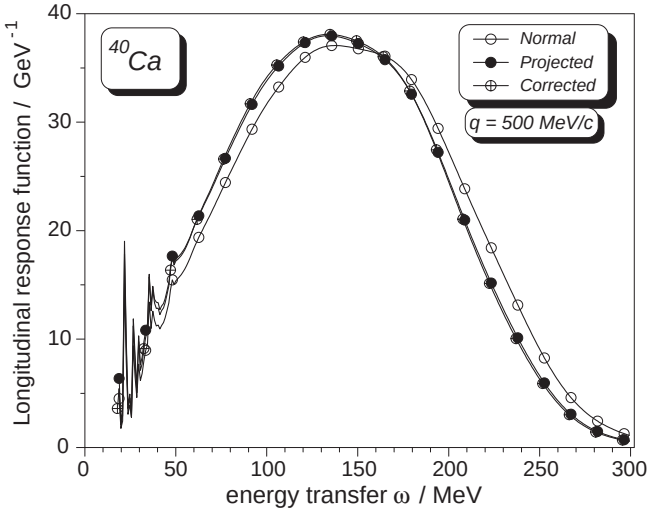

Fig. 4. Same as in fig. 1 but for the nucleus ^{40}Ca. Again no experimental data are available.

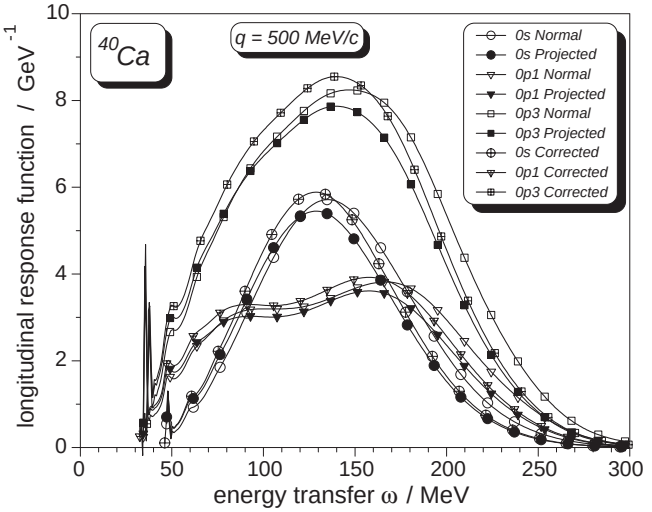

Fig. 5. The longitudinal response of ^{40}Ca to inelastic electron scattering at the 3-momentum transfer $q = 500$ MeV/c out of fig. 4 is decomposed into the various contributions from the $0s$ and $0p$ proton-hole states (the contributions of the neutron-hole states are almost negligible). As before, open symbols refer to the "normal", full symbols to the "projected" and crossed symbols to the "corrected" results.

the neutron hole states are rather small, only the proton hole states have been considered here. It is clearly seen that for this partial response functions the corrected spectral-function approximation yields still the correct peak positions and shapes of the full Galilei-invariant response functions; however, the total strengths are not correctly reproduced. This is to be expected from the spectroscopic factors entering the squares of the form factor functions presented in chapter 2. Consequently the corrected spectral-function approximation overestimates the strength of the $0s$ hole, while it underestimates that of the $0p$ holes. Since for both normal and projected spectroscopic factor the same sum rule holds, this effect is not seen in the total longitudinal response functions displayed in fig. 2 but is clearly present in the exclusive functions shown in fig. 3.

Similar features are obtained for ^{40}Ca. Here, as expected from the larger mass number, the shift in the maximum from the normal (137.7 MeV) to the projected description (133.8 MeV) amounts only to 4 MeV as can be seen from fig. 4. Without nucleon form factor we get here in the normal approximation 19.55 for the Coulomb sum rule, 140.1 MeV for the most probable energy loss and 57.8 MeV for the width, while with projection the corresponding numbers are 19.59, 133.8 MeV and 56.2 MeV, respectively. Here $133.1(1 + 1/40 + 1/39)$ is 139.8 and we are in the simple knock-out model quite near to the quasi-elastic limit. Again the Galilei-invariant total longitudinal response function is reproduced very well by the corrected spectral-function approximation.

However, as already in ^{16}O, differences are seen if particular hole states are considered. Again, there is an overestimation of the strengths of the deep-lying hole states ($0s$ and $0p$ holes, displayed in fig. 5), while for the holes out of the last occupied $1s0d$-shell (fig. 6) the corrected spectral-function approach underestimates the strengths as expected from the spectroscopic factors (2.20).

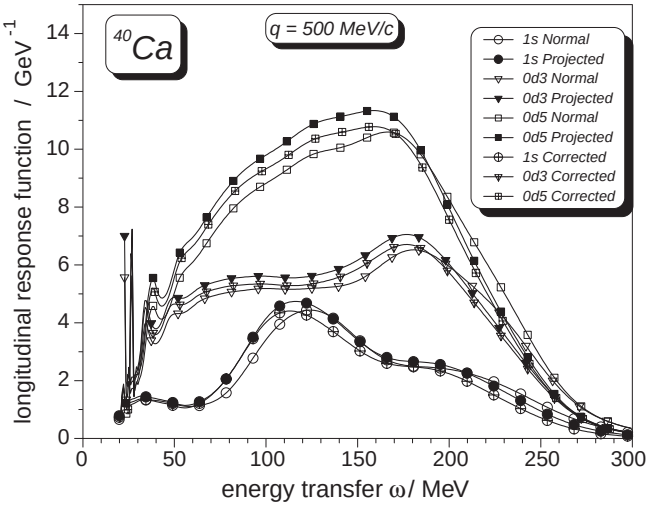

Fig. 6. Same as in fig. 5 but for the proton-hole states from the $1s0d$-shell. The nomenclature is the same as in the previous figures.

4 Conclusions

In the present paper we have analysed the effects of the restoration of Galilei invariance for many-nucleon states with one nucleon in the continuum using as example the longitudinal response function obtained for quasi-elastic electron scattering from ^{4}He, ^{16}O and ^{40}Ca within a simple knock-out model.

For this purpose the target ground states were approximated by simple oscillator determinants in the normal approach which were projected into the COM rest frame in the Galilei-invariant description. For the states of the residual bound system simple one-hole states with respect

to these determinants (again projected into the COM rest frame in the invariant description) were taken. For the continuum nucleon in both approaches a Woods-Saxon partial-wave expansion was applied with the recoil as usual being neglected in the normal, but taken into account exactly in the invariant description. Analytic expressions for the various form factor functions entering the expression for the longitudinal response have been given explicitly.

The results may be summerized as follows. First of all there is a shift of the position of the quasi-elastic peak and a decrease in its width when going from the normal to the Galilei-invariant description. Roughly, the normal approach overestimates the most probable energy loss of the electron by a factor of $(1+1/A+1/(A-1))$. The $1/A$ factor comes from the fact that target and residual states are not living in their respective COM rest frames if the normal approach is used. This factor was already obtained discussing the mathematical sum rules in the second [2] of the present series of papers. The $1/(A-1)$ factor comes from the neglect of the recoil in the normal approach. It is absent, if the closure approximation is made as in ref. [2]; however, it occurs if the intermediate scattering states are constructed explicitly as in the present paper. Obviously the shift in the peak position as well as the decrease in the width (here the difference between the normal and the projected kinetic energies of the target system enters [2]) is a clear $1/A$ effect. In ^{40}Ca the shift amounts to only a few MeV.

Furthermore, it turned out that restricting the form factor functions to the spectral-function parts alone and neglecting the additional terms resulting from non-orthogonality and some higher-order effects is an excellent approximation in our simple model, no matter whether the normal or the projected approach is taken. This allows for a rather simple correction of the normal results: if in the normal spectral-function approximation the momentum transfer is quenched by a factor $(A-1)/A$ and, furthermore, *relative* instead of normal wave functions are used for the various hole states, then the resulting "corrected" spectral-function approach reproduces the results of the full Galilei-invariant calculations rather well as long as only the "inclusive" response functions (*i.e.* the sum of the contributions of all the possible hole states) is considered.

If, on the other hand, the "exclusive" data of particular hole states are considered, the agreement is worse. Here, the corrected spectral-function approach still reproduces the positions and shapes of the Galilei-invariant response functions, underestimates, however, the strengths obtained for hole states out of the last occupied shell, while the contributions of the deeper hole states are overestimated considerably. The reason for this behaviour is the occurence of the spectroscopic factors (2.20) in the projected approach which are considerably different from the ones one expects in the normal approximation. Thus, the different picture obtained in [1] for an uncorrelated system of nucleons if Galilei invariance is restored with respect to the usual expectation manifests itself also in the simple knock-out model considered here.

It is an interesting question whether the above statements do only hold in the simple model considered here or whether they stay true even if a more microscopic approach to the scattering problem is used. In the next of the present series of papers, we shall therefore reinvestigate the inelastic electron scattering within a coupled-channel approach using a suitable many-body Hamiltonian to obtain both the bound and the continuum states which are needed.

References

1. K.W. Schmid, Eur. Phys. J. A **12**, 29 (2001), and references therein.
2. K.W. Schmid, Eur. Phys. J. A **13**, 319 (2002), and references therein.
3. K.W. Schmid, Eur. Phys. J. A **14**, 413 (2002), and references therein.
4. M.A. Preston, R.K. Bhaduri, *Structure of the Nucleus* (Addison-Wesley, Reading 1975).
5. A.E.L. Dieperink, T. de Forest, Phys. Rev. C **10**, 543 (1974).
6. K.F. von Reden *et al.*, Phys. Rev. C **41**, 1084 (1990).
7. C. Ciofi degli Atti, Nucl. Phys. A **473**, 267 (1987).